Inorganic Chemistry

pubs.acs.org/IC

Article

Iodenium or Phosphonium: The Ambi-Valent Character of Iodophosphonium Complexes

Kevin Basemann, Kathleen M. Riley, Jennifer J. Becker, and Michel R. Gagné*

Cite This: *Inorg. Chem.* 2022, 61, 17550−17556

Read Online

ACCESS | Metrics & More | Article Recommendations | Supporting Information

ABSTRACT: The ambi-valent character of the P−I bond in iodophosphonium complexes ensures that it can be electrophilic at either P or I. Herein, we use an ensemble of computational tools and methodologies to probe the nature of this ambi-valent bond. Geometric and atomic electron population analyses yielded strong trends between the electron donating ability of the phosphine and the strength and polarity of the P−I bond. Quasi-atomic orbital analysis demonstrated the near homo-polarity of the P−I bond, and energy decomposition analysis calculations demonstrated the ability to tune the polarization of the bond with only mild changes in secondary structural features. Finally, the ambi-valent nature of the P−I bond was demonstrated to follow hard−soft considerations in reactions with nucleophiles, with harder nucleophiles preferentially forming products of addition to P and softer nucleophiles to I.

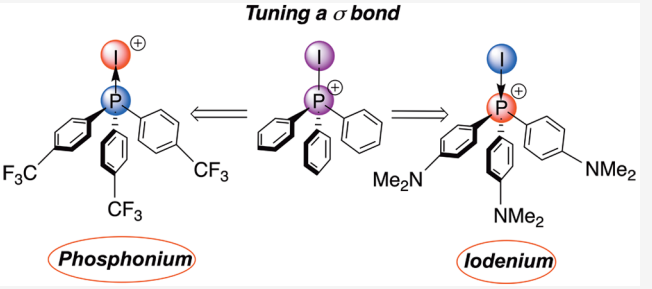

INTRODUCTION

Phosphines (P(III)) are ubiquitous as ligands for catalysts[1−3] and as catalysts themselves.[4−6] In an example of the latter, Stephan has demonstrated the utility of phosphonium cations, P(V), in the catalytic initiation of the hydrosilylation of ketones.[7−9] Exciting examples out of the Radosevich group demonstrate that a P(III)/P(V) redox cycle can be harnessed to accelerate novel reactions.[10−15] Both the Lewis basic properties of P(III) and the Lewis acidic properties of P(V) are demonstrably key components of frustrated Lewis pair chemistry.[16−21] Their broad utility make phosphine catalysis a rich area of research.

Inversion of bond electro- or nucleophilicity, most often through a series of chemical transformations, is a key characteristic of umpolung reactions.[22−27] It stands to reason that learning to subtly control and tune the degree and direction of bond polarization would be enabling for the development of related synthetic methods. Controlling these structure/activity features would benefit from an analysis of compounds with a bond that can be polarized in two directions depending on secondary structural features. The resulting fundamental understanding of this bonding at the electronic level will underpin future developments.

Iodophosphonium iodide compounds (R_3PI_2) have been studied in several reactions, including the iodination of alcohols.[28,29] Several studies have sought to understand the nature of the I−I bond found in the most common "spoke" isomer of these compounds.[30,31] These studies revealed an I−I bond that ranged from covalent (R_3P−I−I) to ion paired [R_3P−I^+][I^-], depending on the particular species or the conditions in which it was synthesized.[32,33] While the I−I bond in iodophosphonium iodide compounds has been well characterized, what is less well studied is the P−I bond. This P−I bond is ideal for studying bond polarization as the electronegativity of P (2.19) and the electronegativity of I (2.66) are relatively close to one another, both are polarizable, and both can be additionally oxidized (Scheme 1).

The known reaction chemistry of the P−I bond in iodophosphonium compounds reveals an ambi-valent (ambi-valent in this work is defined as having multiple valence state interpretations), which makes it a capable source of iodenium (1-coordinate I^+) or phosphonium. This is broadly similar to

Scheme 1. Synthesis, Structure, and Reactivity of Iodophosphonium Compounds

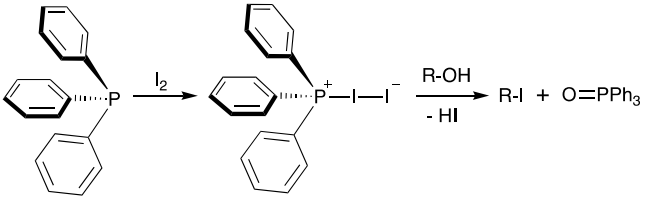

Received: July 18, 2022
Published: October 26, 2022

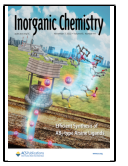

https://doi.org/10.1021/acs.inorgchem.2c02543
Inorg. Chem. 2022, 61, 17550−17556

the umpolung concept; however, the P−I bond expresses both characters simultaneously. Understanding this character advances our goal of fundamentally understanding the reactivity of reagents with ambi-valent properties. In this work, we computationally probe the P−I bonds of iodophosphonium compounds to achieve this.

RESULTS AND DISCUSSION

Computational studies of cationic iodophosphonium complexes were performed to assess their electronic structure and to better define the oxidation state and charges of the P- and I-atoms. These calculations were performed in the NWChem software package[34] using the m06-2x DFT functional[35,36] and the def2-TZVP basis set on all atoms and the associated effective core potential on iodine.[37] Geometry optimizations were confirmed to be in local minima by confirmation that the Hessian calculations had negative frequencies no more than $-100\ cm^{-1}$. Repeated calculations were attempted to eliminate or minimize these negative frequencies to no success; however, calculations run utilizing the B3LYP functional,[38] and subsequent analytical Hessians showed no negative frequencies. Therefore, these negative frequencies may be the result of residuals from non-analytical Hessian calculations rather than deviation from a local minimum. All basis sets in this study were used as defined in the basis set exchange.[39]

The geometry of the calculated iodophosphonium compounds showed the P−I bond length to increase on moving from more electron-poor to more electron-rich phosphine analogues. As the P-substituents become more electron-releasing, the C−P−C angles around phosphorus also shift (slightly) toward an increasingly planar geometry at P. Although these results are subtle, 0.045 Å and 1.4°, respectively (Table 1), the correlation between Hammett constants and ΔP−I and ΔC−P−C are strong ($R^2 > 0.9$). The shift in bond angle is consistent with increasing P(V) character on the phosphorus as the electron density increases, that is, of an increasingly oxidized P (P(III) → P(V)) (Scheme 2).

Table 1. Correlations between Bond Parameters and Charge Based on Phosphine Substituent[a]

para-substituent on aryl groups	C−P−C bond angle (deg)	P−I bond length (Å)	Stone I charge	Stone P−I bond charge
CN	110.2	2.384	0.380	−2.468
CF_3	110.4	2.385	0.361	−2.416
CHO	110.3	2.386	0.345	−2.408
Cl	110.5	2.393	0.321	−2.372
F	110.7	2.394	0.311	−2.391
H	110.7	2.392	0.310	N/A
Me	110.8	2.397	0.278	−2.372
OMe	111.2	2.408	0.245	−2.273
OH	111.0	2.405	0.259	−2.327
NH_2	111.5	2.422	0.181	−2.225
NMe_2	111.6	2.429	0.154	−2.169

[a]Geometry optimizations performed at the m06-2x/def2-tzvp level of theory. Stone charge calculations performed at the HF/Sapporo-TZP/IOTC level of theory.

Another computational tool brought to bear on the problem was Stone multipolar analysis, which provides a quantitative charge and multipole analysis similar to the qualitative insights of Mulliken population analysis.[40−42] Although not explicitly discussed, Stone analysis agrees well with both the Mulliken and Löwdin analyses for the calculations reported herein. The Stone and quasi-atomic orbital (QUAO)[43−45] analyses were performed using the GAMESS software package[46] at the Hartree−Fock level of theory with the infinite-order two-component relativistic method.[47] The Sapporo family of all-electron basis sets were used for all atoms in these calculations; Sapporo-DKH3-TZP-2012 was used for iodine, and Sapporo-TZP-2012 was used for all other atoms.[48] Unsurprisingly, these calculations revealed that the charge on I across the series of PR_3 tends to more positive for more electron-deficient phosphines. Combining this with shorter P−I bond lengths in the same series implied that more electron-deficient phosphines draw electron density from iodine to strengthen/shorten the P−I bond. In contrast, Stone analyses of the charge on P revealed no trend across the Hammett series, implying that increasing charge transfer from I to P effectively buffers the inherent charge on P. Since Stone analysis can also be used to compare the electron population at a defined point in space, it was used to determine the electron population at the center of mass of the P−I vector. Consistent with a strengthening of the P−I bond, its electron population increased for more electron-poor phosphines. Even though I is the more electronegative element, we rationalize that its higher polarizability facilitates electron flow from I to P (i.e., I → P+) when P is more electron-deficient. Stone analysis therefore supports the P(V) + I^- formulation of the oxidation states as being a contributor to the electron structure in addition to the P(III) + I^+ formulation.

Scheme 2. Structural Changes with PR_3 Electronic Withdrawing/Donating Ability

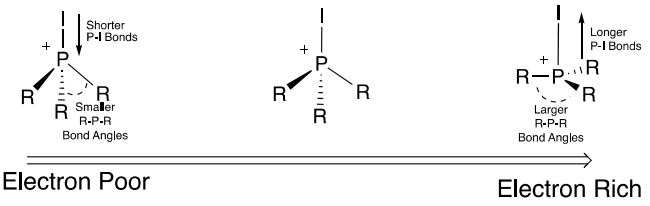

To additionally help define the nature and occupancy of the P−I bond in this series, QUAO analysis was employed. This qualitative method projects localized bonding MOs onto QUAOs and permits one to define both the occupancy of the QUAOs produced and a bond order. The Gordon group previously used this method to help characterize bonding and distinguish between a more polarized electron structure and a less polarized electronic structure. In the case of the iodophosphonium P−I bonds, the method revealed a near equal split in the electron occupation between I and P atoms with a consistently slightly higher occupation on I. As revealed in the Hammett plot (Figure 1), the electron occupation at P remains largely unchanged at the expense of I as one shifts to more electron-poor PR_3 substituents. This trend, along with the bond order being greater than 0.95 in all cases, describes a nearly homopolar P−I covalent bond. Three further observations emerge from analysis of the QUAOs; the first is the trend in the relative strength of the P−I bond, which can be estimated by the kinetic energy term produced in this methodology (Table S1). These revealed a stronger P−I bond for electron-deficient P centers, consistent with observations of the electron occupation of these bonds from Stone analysis. Second, the summation of electron occupation on the P−I bond is consistently slightly greater than 2, suggesting that

https://doi.org/10.1021/acs.inorgchem.2c02543
Inorg. Chem. 2022, 61, 17550−17556

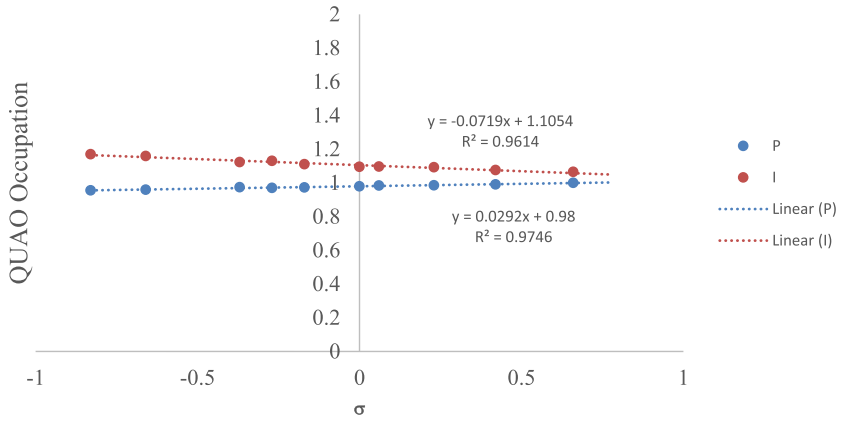

Figure 1. QUAO occupation, the electron occupation on either P or I QUAO calculated for the P−I bond, as a function of Hammett constant. QUAO calculations performed at the HF/Sapporo-TZP/IOTC level of theory.

electron density is being "borrowed" from other orbitals, in this case the lone pair orbitals on I. Finally, the trend that for Ps with strong electron-donating substituents there is more occupation of I and less on P (i.e., R_3P^{2+}/I^-) suggests a more stabilized P(V) formulation.

The homopolar nature of the P−I bond in these species is further supported by their incongruence with the related species, trimethylsilylphosphonium, *N*-iodosuccinimide, and triphenylphosphine oxide. These compounds were chosen to represent a unique four-coordinate phosphonium species, bonding in a well-established iodenium reagent, and bonding in a well-established P(V) species, respectively. In the case of trimethylsilylphosphonium, the P−Si bond order (0.88) is smaller than that of any of the iodophosphonium complexes (P−I > 0.95). Even more telling for a non-homopolar bond are QUAO-derived occupation values, which placed the occupation on silicon at only 0.70, significantly less than the 1.10 observed at I for calculated P−I examples. For *N*-iodosuccinimide, the bond order (0.92) was similar to that of the iodophosphonium complexes, but the occupation value on I (0.69) revealed a bond polarization similar to the trimethylsilylphosphonium case. Finally, triphenylphosphine oxide provided occupation values, P (0.64) and O (1.38), unsurprisingly denoting a polarized σ component of the bond. The comparison of the iodophosphonium species and the comparison set reinforces the uniqueness of the near homogeneous polarization of the P−I bond (Figure 2). The lower occupation number on P in the P−I bond suggests a more positively polarized bond at P than would be expected for a P(III) derivative as evidenced by comparison to the trimethylsilylphosphonium case. On the other hand, the comparison to triphenylphosphine oxide suggests that the bond is also less polarized than a P(V) analogue. The resulting

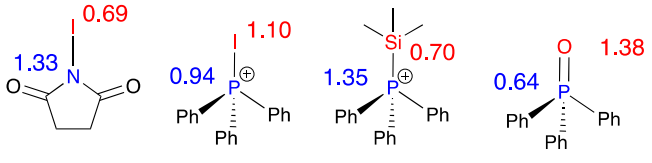

Figure 2. Electron occupation of QUAOs across the N−I bond in *N*-iodosuccinimide, the P−I bond in iodo(triphenyl)phosphonium, the Si−P bond in trimethylsilyl(triphenyl)phosphonium, and the P−O in triphenylphosphine oxide. QUAO calculations performed at the HF/Sapporo-TZP/IOTC level of theory.

intermediate P electron population from the P−I bond thus leads to a homogeneous P−I bond polarization in the iodophosphonium compounds.

It was also desirable to obtain a semi-quantitative assessment of iodenium versus phosphonium character. This was achieved by the development of a method originally stimulated by the work of Djukic et al. in determining the silylicity of metal-silyl complexes.[49] In the current approach, energy decomposition analysis (EDA)[50] calculations were performed twice on the same molecule, heterolytically splitting the electrons of the P−I bond in both potential electronic fragments, that is, $[P^{2+} + I^-]$ and $[P + I^+]$. The former represents a P(V) phosphonium situation, and the latter represents a P(III) iodenium. Comparing these EDA energies gave a semi-quantitative measure of the favorability of splitting the electrons one way versus the other. That is, if the P and I^+ analogue's interaction energy is smaller than the P^{2+} and I^- analogue, then the former is the more stable bond polarization and vice versa. As a proof of concept, this method was applied to an ionic example where the splitting of the electrons is well defined. In this case, LiI was calculated as both the Li^+ and I^- and Li^- and I^+ fragments. This gave an interaction energy of −134.78 kcal/mol for the Li^+/I^- fragments and −341.76 kcal/mol for the mismatched Li^-/I^+ electronic arrangement. It holds then that applying eq 1 to these calculations leads to a value greater than 0, thereby indicating that the lower energy heterolytic splitting of electrons on Li and I fragments is as Li^+ and I^-

$$\Delta E_{\mathrm{Int}}^{\mathrm{Li{+}{+}I{-}}} - \Delta E_{\mathrm{Int}}^{\mathrm{Li{-}{+}I{+}}} > 0 \qquad (1)$$

Applying this same methodology to the P−I bond in the iodophosphoniums provides the means to independently assess which heterolytic splitting of the P−I electrons is most favorable and by extension whether the compound has more iodenium or phosphonium character. Triphenylphosphonium iodide, for example, favored the Ph_3P/I^+ interaction with the difference between the interactions (*I*, eq 2) being 69.5 kcal/mol. In more electron-deficient iodophosphonium species, *I* increased, suggesting a stronger preference for the R_3P/I^+ interaction, that is, more iodenium character. More electron-rich iodophosphonium species decreased *I*, and for the most electron-rich species, *I* dropped below 0, implying an inversion in favorability, now toward the R_3P^{2+}/I^- formulation. This inversion with only subtle changes in PR_3 is a consequence of the near homopolar nature of the P−I bond. This tunability is notable not only in the fact that it exists, but

https://doi.org/10.1021/acs.inorgchem.2c02543
Inorg. Chem. 2022, 61, 17550−17556

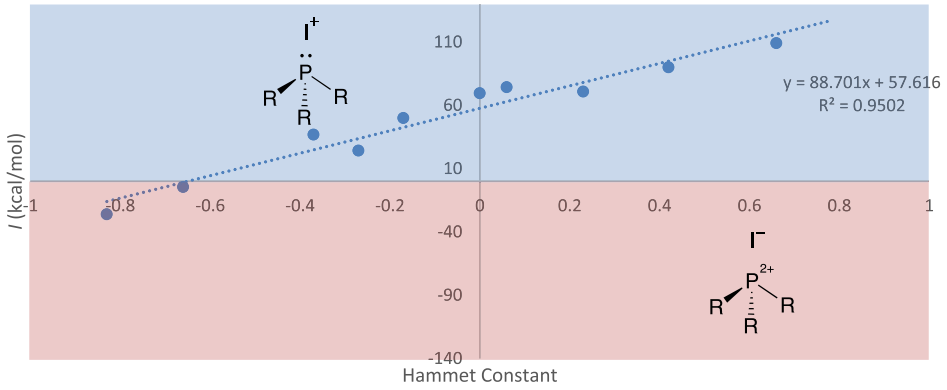

Figure 3. Hammett plot of I (defined in eq 2) depicting a preference for the EDA splitting electrons into either R_3P/I^+ or R_3P^{2+}/I^- fragments. Calculations were performed at the MP2/def2-tzvp level of theory.

also in that it was strong enough to invert the P−I polarization. This is not to say that iodenium could not be abstracted from any of the calculated species; rather, I simply captures the bias of the ambi-valent P−I bond (Figure 3)

$$\Delta E_{\mathrm{Int}}^{\mathrm{P+I+}} - \Delta E_{\mathrm{Int}}^{\mathrm{P2+I-}} = I$$

$$I > 0 \text{ (more iodenium character)}$$

$$I < 0 \text{ (more phosphonium character)} \quad (2)$$

The lowest unoccupied molecular orbital (LUMO) of these compounds is important to our discussion of the bonding between P and I. The LUMO was isolated as part of the valence virtual orbital localization method developed in the GAMESS software package.[51] Unsurprisingly, this revealed the LUMO to be σ^* P−I, which has increased character on I with electron-deficient phosphines and increased character on P for more electron-rich phosphines. However, in all cases, σ^* P−I has considerable antibonding character at both P and I. As shown in Figure 4, the spatial orientation provides a kinetic pathway for adding a nucleophile to either I or P, thus providing the means to experimentally express the ambi-valent character of the P−I bond (Figure 4).

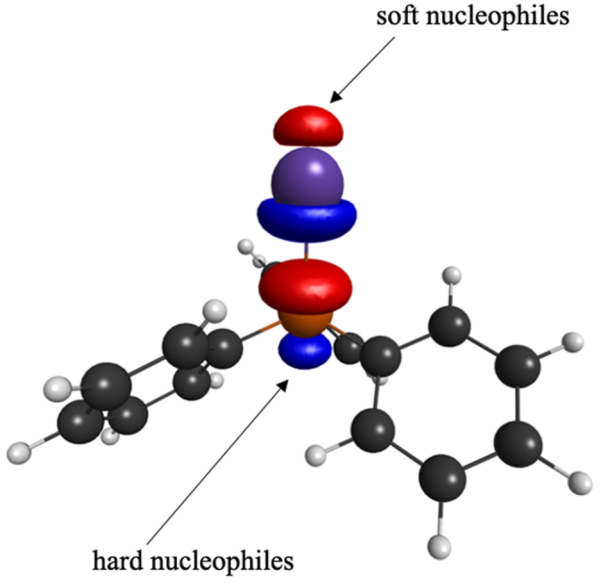

Figure 4. LUMO of Ph_3P-I^+ rendered in MacMolPlt[52] with a contour value of 0.08, with preferential binding of hard/soft nucleophiles annotated. LUMO calculation was performed at the HF/Sapporo-TZP/IOTC level of theory.

Finally, the relative thermodynamic stability of these species was examined by calculating the equilibrium constants for the substitution reaction between an iodophosphonium species and a different phosphine. Whereas previous calculations were performed on the cationic species in the gas phase, the following calculations were performed on species with a BF_4^- counterion in addition to optimizing using the solvation model based on density (SMD) using the parameters for dichloromethane.[53] All other computational details are the same for geometry optimizations of the cationic species. The Gibbs free energies were computed and used to calculate equilibrium constants for various phosphine substitutions (Table 2).

Table 2. Calculated Equilibrium Constants for Substitution of Triphenylphosphine for Triarylphosphine on Iodophosphonium Tetrafluoroborate[a]

$$[Ph_3P\text{-}I][BF_4] \underset{PPh_3}{\overset{PAr_3}{\rightleftharpoons}} [Ar_3P\text{-}I][BF_4] \qquad K_{eq}$$

PAr_3(Ar = C_6H_4X)	K_{eq}
4-CN	2.63×10^{-7}
4-CHO	1.35×10^{-6}
4-Cl	1.35×10^{-2}
4-CF_3	2.94×10^{-7}
4-F	1.07
4-Me	5.46×10^{1}
4-OCH_3	1.31×10^{5}
4-OH	2.96×10^{3}
4-NH_2	2.40×10^{6}
4-NMe_2	2.42×10^{7}
2-Me	2.18×10^{6}
2-*i*Pr	6.33×10^{12}

[a]Equilibrium constants calculated at the m06-2x/def2-tzvp/SMD-(DCM) level of theory.

Unsurprisingly, iodophosphoniums with electron-rich phosphines were thermodynamically preferred to electron-poor phosphines, a reasonable consequence of stabilizing a cationic species (e.g., Scheme 3). More interesting, however, were the large steric effects which hindered the P−I bond and undermined a purely electronic thermodynamic stability trend. For example, $(o\text{-}i\mathrm{PrPh})_3P$ was less favorable than even the extremely electron-deficient tris(pentafluorophenyl)-

https://doi.org/10.1021/acs.inorgchem.2c02543
Inorg. Chem. 2022, 61, 17550−17556

Scheme 3. Equilibrium Reaction for Substitution Reaction of Iodotriphenylphosphonium Tetrafluoroborate with Triarylphosphines[a]

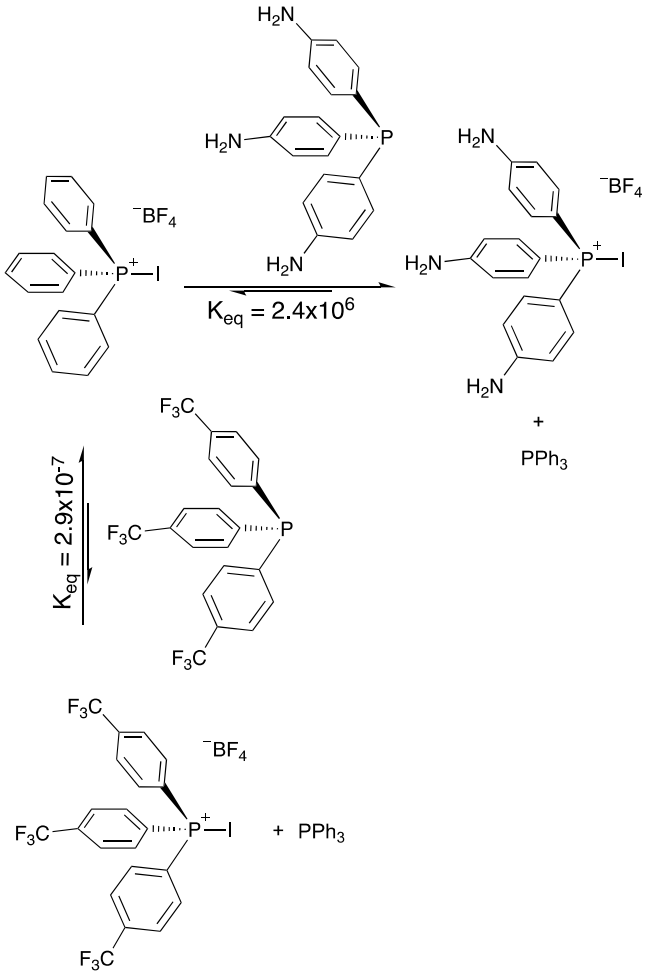

[a]Equilibrium constants calculated at the m06-2x/def2-tzvp/SMD-(DCM) level of theory.

phosphine. Unfortunately, efforts to benchmark these calculations experimentally were hampered by the formation of mixtures of P−I−P$^+$, P′−I−P$^+$, and P′−I−P′$^+$ complexes.

The electronically flexible nature of the P−I bond led to questions about the thermodynamics of competing reactions at P versus I, especially with the LUMO σ^* P−I having character similarly split between I and P facilitating reactivity at either position (Figure 4). We hypothesized that the bifurcative reactivity of P versus I would be influenced by hard−soft considerations, with P preferentially reacting with harder Lewis bases while I would prefer softer Lewis bases. This is born out experimentally on reaction of iodophosphonium with nucleophiles. Soft Lewis bases such as I$^-$ preferentially bind at iodenium (to generate R$_3$P−I−I),[30] whereas in the iodination of alcohols, the reaction proceeds through a step where the alcohol adds to P.[28] Calculations were employed to get a quantitative assessment of the thermodynamics of this phenomenon. Halides (F$^-$, Cl$^-$, Br$^-$, and I$^-$) were used as nucleophiles to span the range from hard (F$^-$) to soft (I$^-$) and calculated as bonding in a linear manner to either I or P in the iodophosphonium complexes. While P binding may be expected to be slightly disfavored due to the greater steric hindrance around P relative to I, it was nevertheless found that binding to P was thermodynamically preferred for all nucleophiles but iodide. Comparison of the relative energies of the isomers revealed the hypothesized trend (Scheme 4).

Scheme 4. Thermodynamic Favorability of Halide Reaction with Iodophosphonium Cation[a]

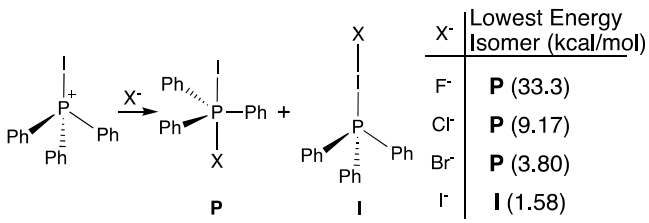

[a]Energy difference calculated at the m06-2x/def2-tzvp/SMD(DCM) level of theory.

When fluoride was bound to iodine (**I**) versus phosphine (**P**), a 33.3 kcal/mol preference for P−F bond formation was observed. For iodine, a 1.6 kcal/mol preference for **I** over **P** was observed. The inversion in thermodynamic **I** versus **P** preference with the hard/soft nature of the halide reinforces the ambi-valent nature of the iodophosphonium species. Anecdotally, these iodophosphonium species are particularly susceptible to reaction with water and alcohols. However, the iodine also reacts readily as an iodenium source with softer nucleophiles such as iodide as evidenced in the spoke structure of the iodophosphonium iodide compounds.

CONCLUSIONS

Iodophosphonium compounds have been found to have an ambi-valent P−I bond. Classic methods of qualitative analysis struggled to adequately define the nature of this bond and predict its observed reactivity. Multiple computational methodologies were employed to reveal a P−I bond that was nearly homopolar in nature. This bond was found to most typically transfer electron density from I to P in variable quantities depending on the P-substituents. Ultimately, the insights provided by the ensemble of methods discussed herein led to the hypothesis, subsequently confirmed by calculation, that the thermodynamics of bond forming around iodophosphonium compounds would be subject to hard−soft considerations, with harder nucleophiles reacting at P and softer at I. This provides insight into the degree to which the polarity of the bond can be tuned using modest secondary structural changes.

ASSOCIATED CONTENT

Supporting Information

The Supporting Information is available free of charge at https://pubs.acs.org/doi/10.1021/acs.inorgchem.2c02543.

Computational methodology and additional data (PDF)
Cartesian coordinates of optimized structures used in this study (XYZ)

AUTHOR INFORMATION

Corresponding Author

Michel R. Gagné − *Caudill Laboratories, Department of Chemistry, University of North Carolina at Chapel Hill, Chapel Hill, North Carolina 27599-3290, United States;* orcid.org/0000-0001-8424-5547; Email: mgagne@unc.edu

https://doi.org/10.1021/acs.inorgchem.2c02543
Inorg. Chem. 2022, 61, 17550−17556

Authors

Kevin Basemann − *Caudill Laboratories, Department of Chemistry, University of North Carolina at Chapel Hill, Chapel Hill, North Carolina 27599-3290, United States;* orcid.org/0000-0001-8203-0112

Kathleen M. Riley − *Caudill Laboratories, Department of Chemistry, University of North Carolina at Chapel Hill, Chapel Hill, North Carolina 27599-3290, United States*

Jennifer J. Becker − *U.S. Army Research Office, Research Triangle Park, North Carolina 27709, United States*

Complete contact information is available at: https://pubs.acs.org/10.1021/acs.inorgchem.2c02543

Notes

The authors declare no competing financial interest.

■ ACKNOWLEDGMENTS

K.D.B. would like to thank the National Research Council for Postdoctoral Fellowship, and M.R.G. would like to thank the National Institute of General Medical Science of the National Institutes of Health for support (R01GM130693). The authors thank the University of North Carolina at Chapel Hill and the Research Computing group for providing computational resources and support that have contributed to these research results.

■ REFERENCES

(1) Clevenger, A. L.; Stolley, R. M.; Aderibigbe, J.; Louie, J. Trends in the Usage of Bidentate Phosphines as Ligands in Nickel Catalysis. *Chem. Rev.* **2020**, *120*, 6124−6196.

(2) Christian, A. H.; Niemeyer, Z. L.; Sigman, M. S.; Toste, F. D. Uncovering Subtle Ligand Effects of Phosphines Using Gold(I) Catalysis. *ACS Catal.* **2017**, *7*, 3973−3978.

(3) Niemeyer, Z. L.; Milo, A.; Hickey, D. P.; Sigman, M. S. Parameterization of Phosphine Ligands Reveals Mechanistic Pathways and Predicts Reaction Outcomes. *Nat. Chem.* **2016**, *8*, 610−617.

(4) Kamijo, S.; Kanazawa, C.; Yamamoto, Y. Copper- or Phosphine-Catalyzed Reaction of Alkynes with Isocyanides. Regioselective Synthesis of Substituted Pyrroles Controlled by the Catalyst. *J. Am. Chem. Soc.* **2005**, *127*, 9260−9266.

(5) Wallace, D. J.; Sidda, R. L.; Reamer, R. A. Phosphine-Catalyzed Cycloadditions of Allenic Ketones: New Substrates for Nucleophilic Catalysis. *J. Org. Chem.* **2007**, *72*, 1051−1054.

(6) Chung, Y. K.; Fu, G. C. Phosphine-Catalyzed Enantioselective Synthesis of Oxygen Heterocycles. *Angew. Chem., Int. Ed.* **2009**, *48*, 2225−2227.

(7) Süsse, L.; LaFortune, J. H. W.; Stephan, D. W.; Oestreich, M. Axially Chiral, Electrophilic Fluorophosphonium Cations: Synthesis, Lewis Acidity, and Reactivity in the Hydrosilylation of Ketones. *Organometallics* **2019**, *38*, 712−721.

(8) Pérez, M.; Qu, Z.-W.; Caputo, C. B.; Podgorny, V.; Hounjet, L. J.; Hansen, A.; Dobrovetsky, R.; Grimme, S.; Stephan, D. W. Hydrosilylation of Ketones, Imines and Nitriles Catalysed by Electrophilic Phosphonium Cations: Functional Group Selectivity and Mechanistic Considerations. *Chem.—Eur. J.* **2015**, *21*, 6491−6500.

(9) Mehta, M.; Holthausen, M. H.; Mallov, I.; Pérez, M.; Qu, Z.-W.; Grimme, S.; Stephan, D. W. Catalytic Ketone Hydrodeoxygenation Mediated by Highly Electrophilic Phosphonium Cations. *Angew. Chem., Int. Ed.* **2015**, *54*, 8250−8254.

(10) Li, G.; Kanda, Y.; Hong, S. Y.; Radosevich, A. T. Enabling Reductive C-N Cross-Coupling of Nitroalkanes and Boronic Acids by Steric Design of P(III)/P(V)=O Catalysts. *J. Am. Chem. Soc.* **2022**, *144*, 8242−8248.

(11) Nykaza, T. V.; Cooper, J. C.; Li, G.; Mahieu, N.; Ramirez, A.; Luzung, M. R.; Radosevich, A. T. Intermolecular Reductive C-N Cross Coupling of Nitroarenes and Boronic Acids by P^{III}/P^{V}=O Catalysis. *J. Am. Chem. Soc.* **2018**, *140*, 15200−15205.

(12) Li, G.; Qin, Z.; Radosevich, A. T. P(III)/P(V)-Catalyzed Methylamination of Arylboronic Acids and Esters: Reductive C-N Coupling with Nitromethane as a Methylamine Surrogate. *J. Am. Chem. Soc.* **2020**, *142*, 16205−16210.

(13) Wang, S. R.; Radosevich, A. T. $P(NMe_2)_3$-Mediated Umpolung Alkylation and Nonylidic Olefination of α-Keto Esters. *Org. Lett.* **2015**, *17*, 3810−3813.

(14) Zhao, W.; Fink, D. M.; Labutta, C. A.; Radosevich, A. T. A $C_{sp}^3-C_{sp}^3$ Bond Forming Reductive Condensation of α-Keto Esters and Enolizable Carbon Pronucleophiles. *Org. Lett.* **2013**, *15*, 3090−3093.

(15) Ghosh, A.; Lecomte, M.; Kim-Lee, S.; Radosevich, A. T. Organophosphorus-Catalyzed Deoxygenation of Sulfonyl Chlorides: Electrophilic (Fluoroalkyl)Sulfenylation by P^{III}/P^{V} =O Redox Cycling. *Angew. Chem., Int. Ed.* **2019**, *58*, 2864−2869.

(16) Shirakawa, S.; Tokuda, T.; Kasai, A.; Maruoka, K. Design of Chiral Bifunctional Quaternary Phosphonium Bromide Catalysts Possessing an Amide Moiety. *Org. Lett.* **2013**, *15*, 3350−3353.

(17) Pérez, M.; Mahdi, T.; Hounjet, L. J.; Stephan, D. W. Electrophilic Phosphonium Cations Catalyze Hydroarylation and Hydrothiolation of Olefins. *Chem. Commun.* **2015**, *51*, 11301−11304.

(18) Stepen, A. J.; Bursch, M.; Grimme, S.; Stephan, D. W.; Paradies, J. Electrophilic Phosphonium Cation-Mediated Phosphane Oxide Reduction Using Oxalyl Chloride and Hydrogen. *Angew. Chem., Int. Ed.* **2018**, *57*, 15253−15256.

(19) Vasko, P.; Zulkifly, I. A.; Fuentes, M. Á.; Mo, Z.; Hicks, J.; Kamer, P. C. J.; Aldridge, S. Reversible C−H Activation, Facile C−B/B−H Metathesis and Apparent Hydroboration Catalysis by a Dimethylxanthene-Based Frustrated Lewis Pair. *Chem. - Eur. J.* **2018**, *24*, 10531−10540.

(20) Dupré, J.; Gaumont, A.-C.; Lakhdar, S. Mechanistic Investigations of Reactions of the Frustrated Lewis Pairs (Triarylphosphines/$B(C_6F_5)_3$) with Michael Acceptors. *Org. Lett.* **2017**, *19*, 694−697.

(21) Chang, K.; Wang, X.; Fan, Z.; Xu, X. Reactions of Neutral Scandium/Phosphorus Lewis Pairs with Small Molecules. *Inorg. Chem.* **2018**, *57*, 8568−8580.

(22) Seebach, D.; Corey, E. J. Generation and Synthetic Applications of 2-Lithio-1,3-Dithianes. *J. Org. Chem.* **1975**, *40*, 231−237.

(23) Seebach, D. Methods of Reactivity Umpolung. *Angew. Chem., Int. Ed. Engl.* **1979**, *18*, 239−258.

(24) Maddigan-Wyatt, J. T.; Cao, J.; Ametovski, J.; Hooper, J. F.; Lupton, D. W. Enantioselective Synthesis of Pyrrolidines by a Phosphine-Catalyzed γ-Umpolung/β-Umpolung Cascade. *Org. Lett.* **2022**, *24*, 2847−2852.

(25) Kishi, K.; Takizawa, S.; Sasai, H. Phosphine-Catalyzed Dual Umpolung Domino Michael Reaction: Facile Synthesis of Hydroindole- and Hydrobenzofuran-2-Carboxylates. *ACS Catal.* **2018**, *8*, 5228−5232.

(26) Zhang, K.; Cai, L.; Hong, S.; Kwon, O. Phosphine-Catalyzed α-Umpolung-Aldol Reaction for the Synthesis of Benzo[b]azapin-3-ones. *Org. Lett.* **2019**, *21*, 5143−5146.

(27) Fan, Y. C.; Kwon, O. Advances in Nucleophilic Phosphine Catalysis of Alkenes, Allenes, Alkynes, and MBHADs. *Chem. Commun.* **2013**, *49*, 11588.

(28) Johnson, R. A.; Herr, M. E. Formation of (Alkoxymethylene)-Dimethylimmonium Halides in the Reactions of Triphenylphosphine Dihalides with Alcohols in Dimethylformamide. *J. Org. Chem.* **1972**, *37*, 310−312.

(29) Verheyden, J. P. H.; Moffatt, J. G. Direct Iodination of the Sugar Moiety in Nucleosides. *J. Am. Chem. Soc.* **1964**, *86*, 2093−2095.

(30) Godfrey, S. M.; Kelly, D. G.; McAuliffe, C. A.; Mackie, A. G.; Pritchard, R. G.; Watson, S. M. The structure of triphenylphosphorus-diiodine, Ph3PI2, the first crystallographically characterised dihalogen derivative of a tertiary phosphine. *J. Chem. Soc., Chem. Commun.* **1991**, *17*, 1163−1164.

(31) Borys, A. M.; Clark, E. R. Adducts of Donor-Functionalized Ar3P with the Soft Lewis Acid I2: Probing Simultaneous Lewis

Acidity and Basicity at Internally Solvated P(III) Centers. *Inorg. Chem.* **2017**, *56*, 4622−4634.
(32) Núñez, R.; Teixidor, F.; Kivekäs, R.; Sillanpää, R.; Viñas, C. Influence of the solvent and R groups on the structure of (carboranyl)R2PI2 compounds in solution. Crystal structure of the first iodophosphonium salt incorporating the anion [7,8-nido-C2B9H10]−. *Dalton Trans.* **2008**, *11*, 1471.
(33) Barnes, N. A.; Godfrey, S. M.; Khan, R. Z.; Pierce, A.; Pritchard, R. G. A Structural and Spectroscopic Study of Tris-Aryl Substituted R3PI2 Adducts. *Polyhedron* **2012**, *35*, 31−46.
(34) Aprà, E.; Bylaska, E. J.; de Jong, W. A.; Govind, N.; Kowalski, K.; Straatsma, T. P.; Valiev, M.; van Dam, H. J. J.; Alexeev, Y.; Anchell, J.; Anisimov, V.; Aquino, F. W.; Atta-Fynn, R.; Autschbach, J.; Bauman, N. P.; Becca, J. C.; Bernholdt, D. E.; Bhaskaran-Nair, K.; Bogatko, S.; Borowski, P.; Boschen, J.; Brabec, J.; Bruner, A.; Cauët, E.; Chen, Y.; Chuev, G. N.; Cramer, C. J.; Daily, J.; Deegan, M. J. O.; Dunning, T. H.; Dupuis, M.; Dyall, K. G.; Fann, G. I.; Fischer, S. A.; Fonari, A.; Früchtl, H.; Gagliardi, L.; Garza, J.; Gawande, N.; Ghosh, S.; Glaesemann, K.; Götz, A. W.; Hammond, J.; Helms, V.; Hermes, E. D.; Hirao, K.; Hirata, S.; Jacquelin, M.; Jensen, L.; Johnson, B. G.; Jónsson, H.; Kendall, R. A.; Klemm, M.; Kobayashi, R.; Konkov, V.; Krishnamoorthy, S.; Krishnan, M.; Lin, Z.; Lins, R. D.; Littlefield, R. J.; Logsdail, A. J.; Lopata, K.; Ma, W.; Marenich, A.V.; Martin del Campo, J.; Mejia-Rodriguez, D.; Moore, J. E.; Mullin, J. M.; Nakajima, T.; Nascimento, D. R.; Nichols, J. A.; Nichols, P. J.; Nieplocha, J.; Otero-de-la-Roza, A.; Palmer, B.; Panyala, A.; Pirojsirikul, T.; Peng, B.; Peverati, R.; Pittner, J.; Pollack, L.; Richard, R. M.; Sadayappan, P.; Schatz, G. C.; Shelton, W. A.; Silverstein, D. W.; Smith, D. M. A.; Soares, T. A.; Song, D.; Swart, M.; Taylor, H. L.; Thomas, G. S.; Tipparaju, V.; Truhlar, D. G.; Tsemekhman, K.; Van Voorhis, T.; Vázquez-Mayagoitia, Á.; Verma, P.; Villa, O.; Vishnu, A.; Vogiatzis, K. D.; Wang, D.; Weare, J. H.; Williamson, M. J.; Windus, T. L.; Woliński, K.; Wong, A. T.; Wu, Q.; Yang, C.; Yu, Q.; Zacharias, M.; Zhang, Z.; Zhao, Y.; Harrison, R. NWChem: Past, present, and future. *J. Chem. Phys.* **2020**, *152*, 184102.
(35) Zhao, Y.; Truhlar, D. G.; Zhao, Y.; Truhlar, D. G. The M06 suite of density functionals for main group thermochemistry, thermochemical kinetics, noncovalent interactions, excited states, and transition elements: two new functionals and systematic testing of four M06-class functionals and 12 other functionals. *Theor. Chem. Acc.* **2008**, *120*, 215−241.
(36) Zhao, Y.; Truhlar, D. G. Density Functionals with Broad Applicability in Chemistry. *Acc. Chem. Res.* **2008**, *41*, 157−167.
(37) Gulde, R.; Pollak, P.; Weigend, F. Error-Balanced Segmented Contracted Basis Sets of Double-ζ to Quadruple-ζ Valence Quality for the Lanthanides. *J. Chem. Theory Comput.* **2012**, *8*, 4062−4068.
(38) Becke, A. D. Density-functional thermochemistry. III. The role of exact exchange. *J. Chem. Phys.* **1993**, *98*, 5648−5652.
(39) Pritchard, B. P.; Altarawy, D.; Didier, B.; Gibson, T. D.; Windus, T. L. New Basis Set Exchange: An Open, Up-to-Date Resource for the Molecular Sciences Community. *J. Chem. Inf. Model.* **2019**, *59*, 4814−4820.
(40) Stone, A. J. Distributed Multipole Analysis, or How to Describe a Molecular Charge Distribution. *Chem. Phys. Lett.* **1981**, *83*, 233−239.
(41) Stone, A. J. Distributed Multipole Analysis: Stability for Large Basis Sets. *J. Chem. Theory Comput.* **2005**, *1*, 1128−1132.
(42) Stone, A. J.; Alderton, M. Distributed Multipole Analysis. *Mol. Phys.* **1985**, *56*, 1047−1064.
(43) Schoendorff, G.; Ruedenberg, K.; Gordon, M. S. Multiple Bonding in Rhodium Monoboride. Quasi-Atomic Analyses of the Ground and Low-Lying Excited States. *J. Phys. Chem. A* **2021**, *125*, 4836−4846.
(44) Schoendorff, G.; West, A. C.; Schmidt, M. W.; Ruedenberg, K.; Wilson, A. K.; Gordon, M. S. Relativistic ab Initio Accurate Atomic Minimal Basis Sets: Quantitative LUMOs and Oriented Quasi-Atomic Orbitals for the Elements Li-Xe. *J. Phys. Chem. A* **2017**, *121*, 3588−3597.
(45) West, A. C.; Duchimaza-Heredia, J. J.; Gordon, M. S.; Ruedenberg, K. Identification and Characterization of Molecular Bonding Structures by Ab Initio Quasi-Atomic Orbital Analyses. *J. Phys. Chem. A* **2017**, *121*, 8884−8898.
(46) Barca, G. M. J.; Bertoni, C.; Carrington, L.; Datta, D.; De Silva, N.; Deustua, J. E.; Fedorov, D. G.; Gour, J. R.; Gunina, A. O.; Guidez, E.; Harville, T.; Irle, S.; Ivanic, J.; Kowalski, K.; Leang, S. S.; Li, H.; Li, W.; Lutz, J. J.; Magoulas, I.; Mato, J.; Mironov, V.; Nakata, H.; Pham, B. Q.; Piecuch, P.; Poole, D.; Pruitt, S. R.; Rendell, A. P.; Roskop, L. B.; Ruedenberg, K.; Sattasathuchana, T.; Schmidt, M. W.; Shen, J.; Slipchenko, L.; Sosonkina, M.; Sundriyal, V.; Tiwari, A.; Galvez Vallejo, J. L.; Westheimer, B.; Włoch, M.; Xu, P.; Zahariev, F.; Gordon, M. S. Recent Developments in the General Atomic and Molecular Electronic Structure System. *J. Chem. Phys.* **2020**, *152*, 154102.
(47) Barysz, M.; Sadlej, A. J. Infinite-Order Two-Component Theory for Relativistic Quantum Chemistry. *J. Chem. Phys.* **2002**, *116*, 2696−2704.
(48) Noro, T.; Sekiya, M.; Koga, T. Segmented Contracted Basis Sets for Atoms H through Xe: Sapporo-(DK)-NZP Sets (n = D, T, Q). *Theor. Chem. Acc.* **2012**, *131*, 1124.
(49) Binh, D. H.; Milovanović, M.; Puertes-Mico, J.; Hamdaoui, M.; Zarić, S. D.; Djukic, J.-P. Is the R_3Si Moiety in Metal-Silyl Complexes a Z ligand? An Answer from the Interaction Energy. *Chem.—Eur. J.* **2017**, *23*, 17058−17069.
(50) Su, P.; Li, H. Energy Decomposition Analysis of Covalent Bonds and Intermolecular Interactions. *J. Chem. Phys.* **2009**, *131*, 014102.
(51) Schmidt, M. W.; Hull, E. A.; Windus, T. L. Valence Virtual Orbitals: An Unambiguous Ab Initio Quantification of the LUMO Concept. *J. Phys. Chem. A* **2015**, *119*, 10408−10427.
(52) Bode, B. M.; Gordon, M. S. Macmolplt: A Graphical User Interface for GAMESS. *J. Mol. Graphics Modell.* **1998**, *16*, 133−138.
(53) Marenich, A. V.; Cramer, C. J.; Truhlar, D. G. Universal Solvation Model Based on Solute Electron Density and on a Continuum Model of the Solvent Defined by the Bulk Dielectric Constant and Atomic Surface Tensions. *J. Phys. Chem. B* **2009**, *113*, 6378.

https://doi.org/10.1021/acs.inorgchem.2c02543
Inorg. Chem. 2022, 61, 17550−17556